THE ASTROPHYSICAL JOURNAL, 443:L33–L36, 1995 April 10

DISCOVERY AND IMAGING OF A GALACTIC CIRRUS CLOUD WITH THE FAR ULTRAVIOLET SPACE TELESCOPE

LAURI K. HAIKALA AND KALEVI MATTILA
Helsinki University Observatory, P.O. Box 14, FIN-00014, University of Helsinki, Finland
STUART BOWYER, TIMOTHY P. SASSEEN, AND MICHAEL LAMPTON
Center for EUV Astrophysics, University of California at Berkeley, Berkeley, CA 94720
AND
JENS KNUDE
Niels Bohr Institute for Astronomy, Physics and Geophysics, Copenhagen University Observatory, Oester Voldgade 3, DK-1350 Copenhagen, Denmark
Received 1994 April 26; accepted 1995 January 24

ABSTRACT

We present new far-ultraviolet (1400–1800 Å) data concerning a Galactic cirrus cloud G251.2+73.3 near the north Galactic pole obtained with the space-borne imaging telescope FAUST. We obtain a good correlation between the far-ultraviolet (FUV) and *IRAS* 100 μm surface brightnesses, their relation being $I_{\rm FUV} = (128 \pm 3) I_{100\,\mu{\rm m}} - (264 \pm 9)$, where the $I_{\rm FUV}$ flux is given in units of photons s^{-1} cm^{-2} $Å^{-1}$ sr^{-1} and $I_{100\,\mu{\rm m}}$ in MJy sr^{-1}. Using *uvby*Hβ photometry, we get a distance of 120 pc and a visual extinction in the center of the cloud of 0.39 mag corresponding to an extinction of 1.0 mag at 1565 Å. We have performed a multiple scattering calculation for the scattered light using the Monte Carlo method. These calculations provide restrictions on the FUV scattering properties of the interstellar dust.

Subject headings: ISM: clouds — dust extinction — ultraviolet: ISM

1. INTRODUCTION

There is now consensus that most of the diffuse far-ultraviolet (FUV) background in the wavelength range 1300–1800 Å comes from scattering by interstellar dust (Bowyer 1991). Nevertheless, it is still desirable to demonstrate by well-calibrated deep ultraviolet imaging that individual dust clouds, seen by their optical extinction or infrared emission, are also detected by means of their excess FUV (scattered) radiation. Although the extinction properties of the interstellar grains in the FUV are well known, the results concerning their scattering properties still span almost the whole physically available ranges for albedo and scattering asymmetry parameter (Hurwitz, Bowyer, & Martin 1991). What is needed to define the scattering parameters in an unequivocal way is both an image with a sufficiently large field of view and small pixel size that provides a differential measurement and elimination of stars to a faint limit, and a model for interpreting these data.

All studies of the FUV scattering properties of interstellar grains in the general interstellar medium (i.e., outside bright nebulae) have so far been based on the *absolute* intensities of the sky background radiation. In addition, in many cases the photometer field of view has been so large that unresolved starlight has been a major problem. When observing the *differential* surface brightness rising from an individual localized cloud, we are free of, or at least much less dependent on, foreground/background components, such as dark current, atmospheric/geocoronal emissions, or the extragalactic diffuse background.

The FUV background correlates with far-infrared emission from interstellar dust on a large scale (Jakobsen, de Vries, & Paresce 1987; Pérault et al. 1991). It is, however, still important to investigate whether the correlation persists to the scale sizes of individual clouds.

We have obtained a FUV wide-field image of a Galactic cirrus cloud near the north Galactic pole using a space-borne imaging telescope, the Far Ultraviolet Space Telescope (FAUST). In this *Letter* we report these observations and their analysis, representing the first discovery and imaging of an individual Galactic cirrus cloud at far-ultraviolet wavelengths. The UV surface emission within the FAUST image is shown to correlate with *IRAS* 100 μm emission. Our FUV measurements, combined with optical *uvby*Hβ photometry of stars in the same field, provide a restriction on the FUV scattering properties of interstellar dust.

2. OBSERVATIONS, DATA REDUCTION, AND RESULTS

The FAUST telescope was flown as part of the NASA ATLAS-1 mission in 1992 March. The telescope has a bandpass between 1400 and 1800 Å and a 7°.6 field of view. The telescope, the mission, the data acquired, and the image data reduction are described in Bowyer et al. (1993). The FUV image discussed in this *Letter* is target 8 (R.A. $\alpha = 12^{\rm h}2^{\rm m}$, $\delta = 17°.9$; $l = 251°.2$, $b = 73°.3$; exposure time 15 minutes).

The airglow and twilight varied during the exposure and produced a large-scale background gradient to the image. This gradient was approximated by a plane which was fitted through a number of positions in the frame assumed to be free from other than background emission.

The image, after subtraction of the fitted background, is shown in Figure 1 (Plate L7). The average value of this fitted background is 1500 photons s^{-1} cm^{-2} $Å^{-1}$ sr^{-1} (to be called CU [continuum units] below). Considerable variation is seen in the sky brightness in the field. The clearest maximum is seen in the southwest quarter of the image at $\alpha = 11^{\rm h}56^{\rm m}$, $\delta = 16°.3$ (1950.0), or $l = 251°.2$, $b = 73°.3$. This maximum corresponds to a well-defined infrared cirrus cloud (to be called G251.2+73.3)

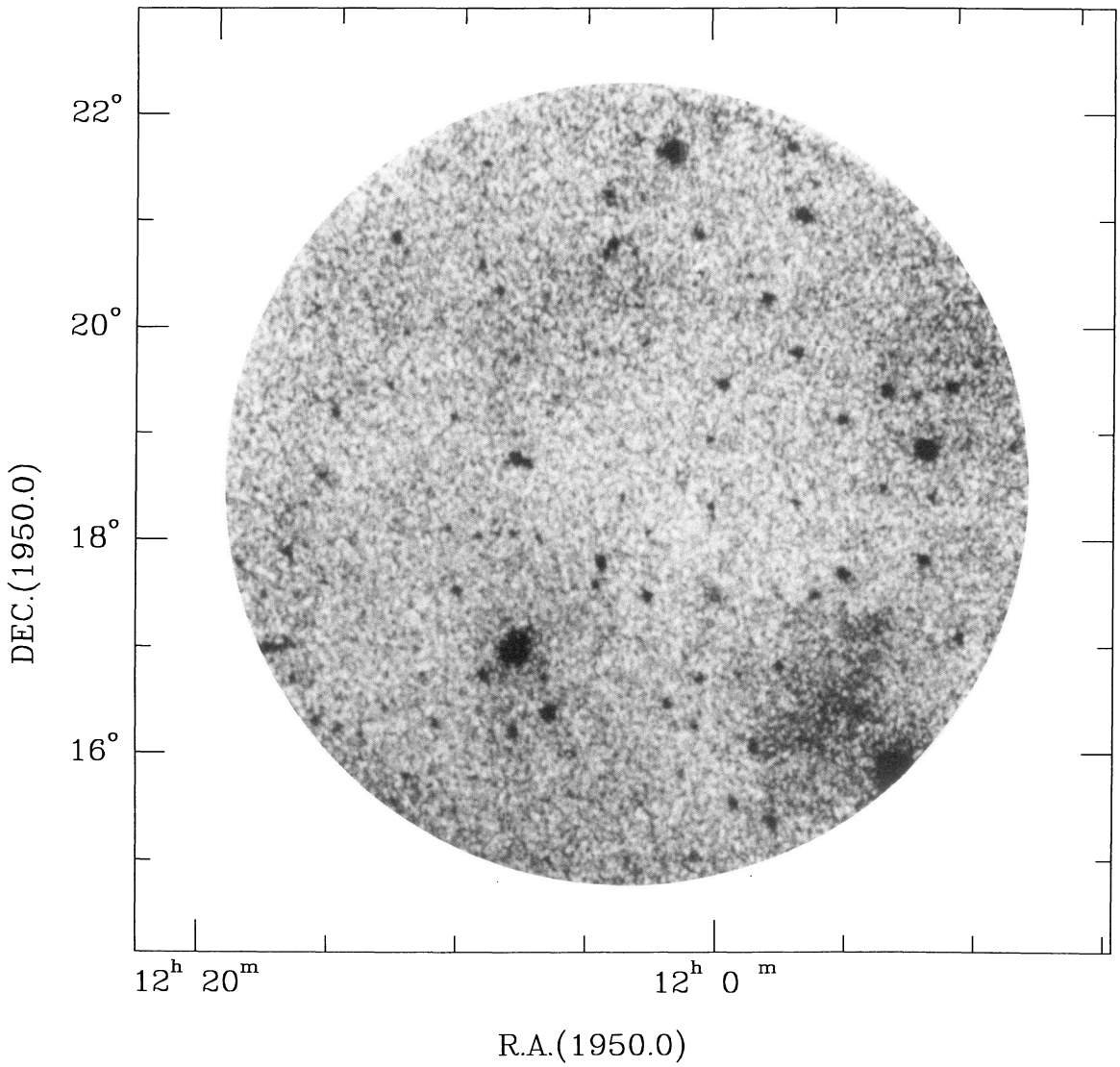

FIG. 1.—FUV (1400–1800 Å) image (negative) of Galactic cirrus obtained with the space-borne imaging telescope FAUST. The maximum surface brightness is 400 CU at the position of G251.2+73.3. The background has been fitted to zero.

HAIKALA et al. (see 443, L33)

seen both on *IRAS* 100 μm (Fig. 2 [Pl. 8]) and on *IRAS* 60 μm maps. The FUV surface brightness above the fitted background at the center of G251.2+73.3 is 410 $\pm$ 60 CU. A fainter surface brightness maximum in the FAUST image at $\alpha = 12^h7^m$, $\delta = 20\overset{\circ}{.}7$ has also a counterpart in the *IRAS* image. The minimum near the center of the FAUST image at $\alpha = 12^h2^m$, $\delta = 18\overset{\circ}{.}5$ is also a minimum in the *IRAS* image.

It is important to establish that the detected UV enhancement feature is not an instrument artifact. First, the FAUST instrument was specifically designed with internal baffling and entrance-aperture stray-light control to guard against veiling flare and spurious low surface brightness images. Second, laboratory scans for stray-light susceptibility were conducted. All 18 of our deep in-flight exposures and scans were searched for stray-light effects. In these scans numerous bright stars transmitted the instrument field of view, while other stars remained outside the field of view. In no case did stray-light artifacts appear. Finally, we have closely examined three very deep fields that have stars of class A or class B as bright as third magnitude within 3° of the field of view. None of these show scattering artifacts or nebulosities. We conclude that the UV enhancement reported here is not an artifact of instrumental glare or stray light but is in fact a unique diffuse emission nebulosity.

3. ANALYSIS

3.1. *uvbyHβ Photometry*

Photometric data in the *uvbyHβ* system are available for ~200 stars in the FAUST field. The photometric data are part of a north Galactic pole (NGP) survey of all A2–G0 stars brighter than $B = 11.5$ mag and with $b \geq 70°$ (Knude 1985). The photometry gives us a relatively densely populated network of stars with known $E(b-y)$ values and distances (about three or four stars per square degree). The sample is volume-complete to a distance of approximately 200 pc. The formal accuracy in one $E(b-y)$ value is 0.006–0.008 mag. The calculated 1 deg^2 averaged $E(b-y)$ values have accordingly a mean error of ~0.005 mag.

A contour map of the 1 deg^2 averaged reddening of starlight in the FAUST field is shown in Figure 3. The contours are lower reddening limits, since the averages include also nearby stars with no or little reddening and lines of sight outside areas containing dust. The position of the FAUST image is indicated with a circle, and the position of the cirrus cloud, $l = 251\overset{\circ}{.}2$, $b = 73\overset{\circ}{.}3$, is marked by a filled square; the FUV maximum falls close to the optical extinction maximum. The qualitative accord with the FAUST and *IRAS* 100 μm intensity distributions is seen to be quite good.

In Figure 4 we have plotted $E(b-y)$ against distance for stars within an approximately 4° × 4° area centered at G251.2 + 73.3 ($11^h45^m < \alpha < 12^h0^m$, $14° < \delta < 18°$). It can be seen that the extinction is very low for $r < 100$ pc. At $r = 120$ pc there is a sharp boundary beyond which several stars have significant extinctions up to $E(b-y) = 0.10$ mag. However, also at $r > 120$ pc most stars have only small extinctions, not distinguishable from $E(b-y) = 0$. This can be understood as due partly to stars visible between clumps in a clumpy cloud area and partly to stars located in the more transparent outskirts of the cloud. The stellar distances have relative errors of ~15%. Negative $E(b-y)$ values are partly statistical and are more frequent for larger distances where only lightly reddened stars were included in the magnitude-limited sample.

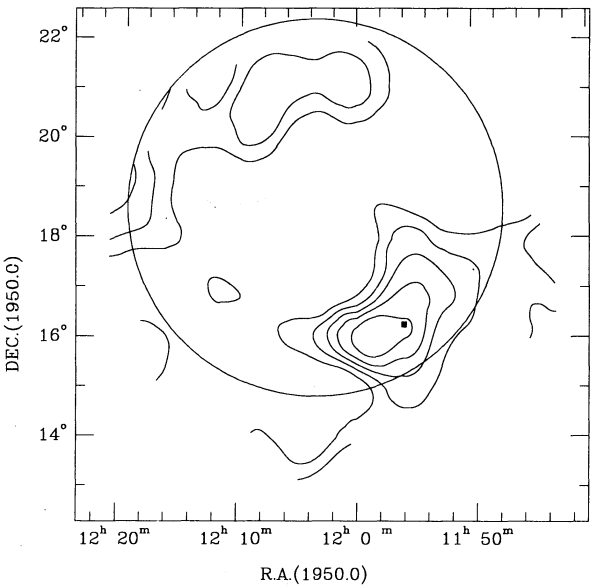

FIG. 3.—Average reddening $E(b-y)$ of starlight in the FAUST field based on the *uvbyHβ* photometry. The position of the FAUST image is indicated with a circle, and the cirrus cloud, $l = 251\overset{\circ}{.}2$, $b = 73\overset{\circ}{.}3$, is marked by a filled square. The contours are from 0.015 to 0.065 mag in steps of 0.01 mag.

These data indicate a distance of about 120 pc for the cloud and a color excess at its center of 0.09 mag, with an estimated error of $\pm$0.02 mag. This corresponds to a visual extinction of $A_V = 4.3E(b-y) = 0.39$ mag and is in good agreement with the estimates obtained from the maximum 100 μm (ON-OFF) intensity of 3.2 MJy sr^{-1} using the $I_{100\,\mu m}/A_V$ conversion coefficients for diffuse clouds (Laureijs, Mattila, & Schnur 1987; Laureijs et al. 1989). Using the standard UV reddening curve (Seaton 1979), the extinction at 1565 Å is 1.0 $\pm$ 0.2 mag.

A bright star, HD 103578, is located about 0°.9 southwest of the center of G251.2+73.3 (see Fig. 1). This star has a spectral type of A3 V, a visual magnitude of 5.50 mag, and a photometric distance of 87 $\pm$ 4 pc (Palous & Hauck 1986). The minimum distance between HD 103578 and G251.2+73.3 is 20 pc, large enough to exclude the star as a significant source of illumination for G251.2+73.3.

3.2. *Correlation of FAUST and IRAS Data*

In order to study the correlation of the FUV and *IRAS* emission, the point sources present in both images had to be

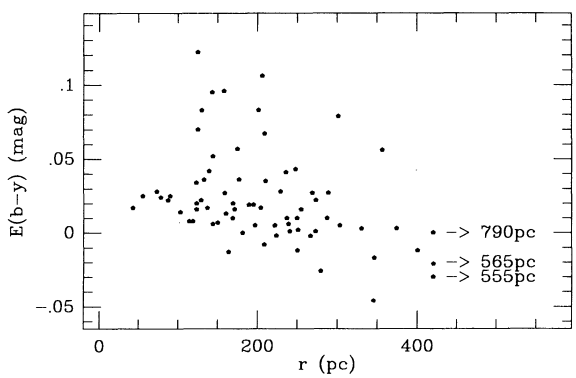

FIG. 4.—Reddening $E(b-y)$ vs. distance for stars in the area of G251.2+73.3

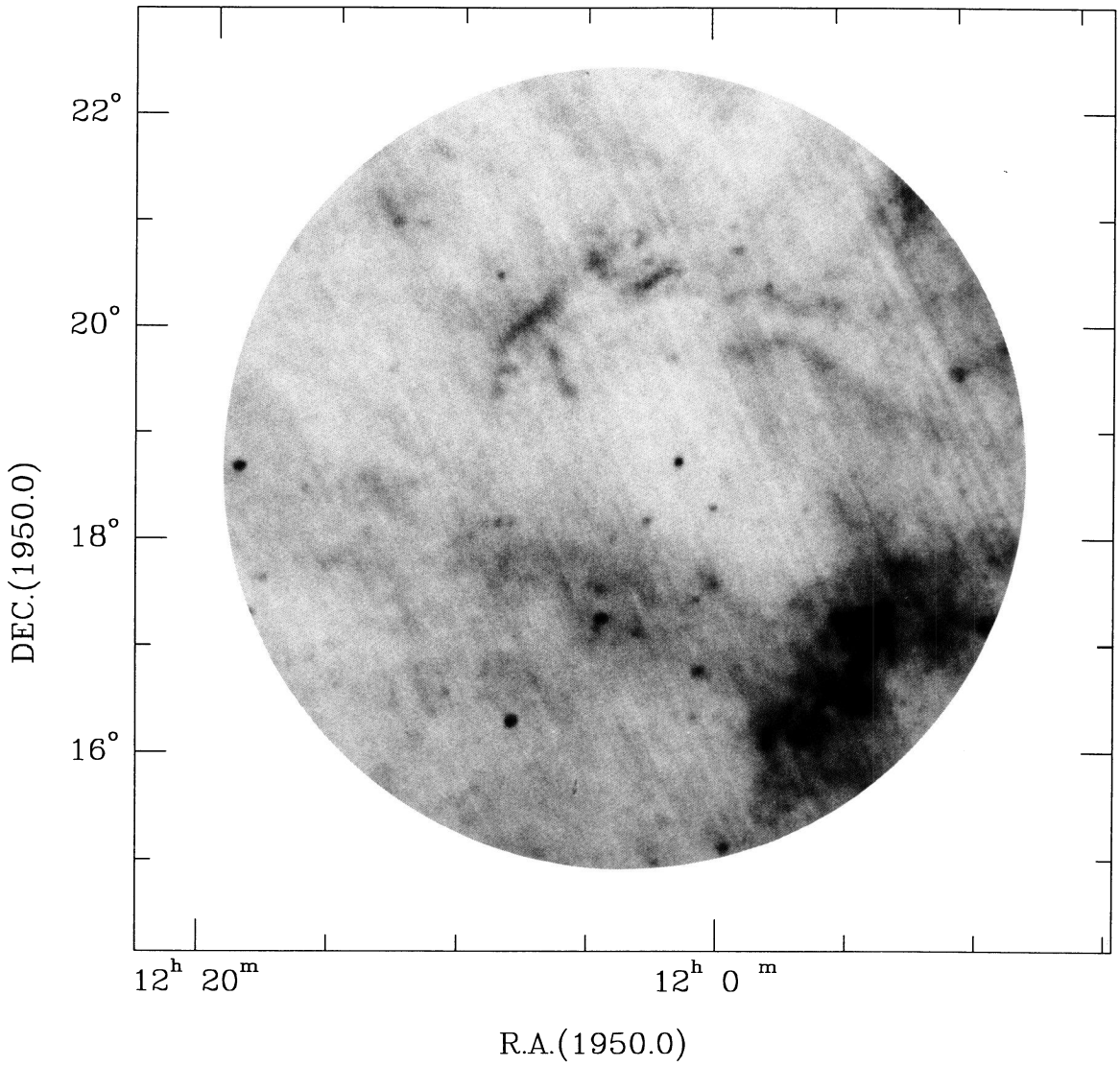

FIG. 2.—*IRAS* (negative) 100 μm image (*IRAS* Sky Survey Atlas field 287) reprojected to the same geometry as the FAUST frame. The maximum surface brightness at the position of G251.2+73.3 is $\sim$8 MJy sr^{-1}, while the background is around 1.5 MJy sr^{-1}.

HAIKALA et al. (see 443, L34)

excluded from the analysis. Point sources in the FAUST image were detected following the procedure given in Sasseen et al. (1994) and blanked out from the image. The strong point sources were blanked out from the *IRAS* image. As the faint, unidentified sources detected only at 100 μm are typical cirrus sources, these were left in place. Since the emission due to zodiacal light has already been removed from the *IRAS* Sky Survey Atlas plates, the 100 μm fluxes were taken from this frame without any further correction. We also rebinned the star-free FAUST image to 4.'5 × 4.'5 pixels, which closely corresponds to the final resolution of the FAUST image (FWHM = 3.'8) and of the *IRAS* 100 μm map (4'–5').

In Figure 5 we plot the FAUST versus *IRAS* 100 μm surface brightness for an area which encompasses the G251.2+73 cirrus cloud area and the adjacent "empty" central area of the FAUST image (see Fig. 1). The cirrus cloud is not a smooth feature but is fragmented into a number of smaller cloudlets. The same fine structure is clearly discernible in both the FAUST and the *IRAS* images. The two brightnesses are clearly correlated. A least-squares solution gives the relationship: $I_{\rm FAUST} = (128 \pm 3) I_{100\,\mu{\rm m}} - 264 \pm 9$ (correlation coefficient $\rho = 0.82$), where $I_{\rm FAUST}$ is in CU and $I_{100\,\mu{\rm m}}$ is MJy sr^{-1}. The constant term has not much physical significance because neither for FAUST nor for the *IRAS* 100 μm map is the absolue zero level known; the zero point has been determined either within the image (FAUST) or is set by a zodiacal emission model (*IRAS* 100 μm map).

Correlation diagrams with slopes similar to that shown in Figure 5 have been obtained for the other portions of the FAUST image, as well as for the whole area of the image. This demonstrates that the conversion coefficient as given above is valid not just for G251.2+73.3 but more generally for the dust in this area.

3.3. *FUV Scattering Model*

The FUV surface brightness of G252.2+73.3 contains a contribution from H_2 fluorescence. G251.2+73.3 has an H I column density of 6.5×10^{20} cm^{-2} (Deul & Burton 1990), which is comparable to the high Galactic latitude targets 2, 6, and 7 in the spectroscopic study of Martin, Hurwitz, & Bowyer (1990). If the FUV spectrum of the cloud differs only in intensity from these targets, we estimate that the contribution of H_2 fluorescence to the FAUST band is 75 ± 15 CU, leaving a surface brightness excess ΔI of 335 ± 75 CU.

We have performed a multiple scattering calculation for the scattered light ($I_{\rm sca}$) in G251.2+73.3 using the Monte Carlo method as described by Mattila (1970). The cloud is modeled as a homogeneous sphere of optical thickness (diameter) of $\tau(1565\ \text{Å}) = 1.0$. The scattering function of a single grain is approximated with the Henyey-Greenstein function (Henyey & Greenstein 1941), characterized by the single scattering albedo a and asymmetry parameter g.

In order to make a comparison with the observed excess surface brightness in G251.2+73.3, we have to consider the effect of an isotropic (or nearly isotropic) background radiation component (Galactic halo + extragalactic) which originates beyond the distance of G251.2+73.3. The isotropic background radiation, I_0, will be shadowed by the cloud, the transmitted component being $I_0 e^{-\tau}$. In addition, the isotropic component is also scattered by the cloud if the albedo a is greater than zero. Denoting the scattered isotropic component by $I_0 f_{\rm sca}$, the depression of the isotropic background radiation in the direction of the cloud is

$$\Delta I_0 = I_0(1 - e^{-\tau} + f_{\rm sca}) = I_0 h\,. \qquad (1)$$

The quantity h has been tabulated for different values of τ, a, and g by Mattila (1976, Appendix, Table A2).

The calculated surface brightness differences (ON-OFF) in CU, $\Delta I_{\rm calc} = I_{\rm sca} - \Delta I_0$ are given in Table 1 for a cloud with optical thickness $\tau(1565\ \text{Å}) = 1.0$, seen in the direction $l = 251.°2$, $b = 73.°3$, exposed to the Galactic FUV integrated starlight (ISL) radiation field at 1565 Å (Gondhalekar 1990) plus isotropic background component I_0 from behind the cloud (halo + extragalactic). The results for two different values of the isotropic background are tabulated, i.e., $I_0 = 0$ CU and $I_0 = 300$ CU. Since only stars brighter than 1×10^{-12} ergs s^{-1} cm^{-2} Å^{-1} are included in this ISL, a correction is needed for the fainter stars and the diffuse Galactic radiation. We followed the procedure as described in Gondhalekar, Phillips, & Wilson (1980). We multiplied the ISL values in the interval $|b| \leq 40°$ by the factor 1.11. This results in an overall increase of the radiation field by 10%, corresponding to the Gondhalekar et al. (1980) case. The average intensity of the resulting

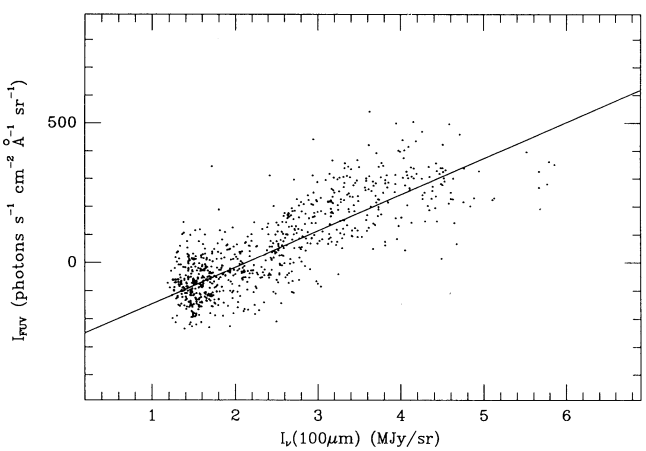

FIG. 5.—Correlation between the FUV (FAUST) and FIR 100 μm (*IRAS*) surface brightness in the area of G251.2+73.3 and an adjacent empty area in the center of the FAUST image (see Fig. 1).

TABLE 1

CALCULATED SURFACE BRIGHTNESS DIFFERENCES

	g				
a	0.00	0.25	0.50	0.75	0.90
			$I_0 = 0$ CU		
0.80.....	3166	3038	2377	1381	585
0.60.....	2181	2073	1577	889	375
0.40.....	1344	1263	933	508	213
0.20.....	624	580	416	218	91
0.10.....	312	290	208	109	45
0.00.....	0	0	0	0	0
			$I_0 = 300$ CU		
0.80.....	3116	2988	2327	1328	532
0.60.....	2088	1980	1483	793	279
0.40.....	1215	1134	803	376	81
0.20.....	504	420	255	56	−71
0.10.....	138	116	34	−66	−130
0.00.....	−187	−187	−187	−187	−187

TABLE 2

BEST-FIT ALBEDO VALUES (a)

I_0 (CU)	g 0.00	0.25	0.50	0.75	0.90
0.....	$0.11^{+0.03}_{-0.05}$	$0.12^{+0.02}_{-0.03}$	$0.16^{+0.04}_{-0.04}$	$0.28^{+0.04}_{-0.05}$	$0.55^{+0.08}_{-0.09}$
115.....	$0.13^{+0.02}_{-0.03}$	$0.14^{+0.02}_{-0.03}$	$0.19^{+0.03}_{-0.03}$	$0.32^{+0.05}_{-0.05}$	$0.60^{+0.06}_{-0.09}$
300.....	$0.15^{+0.02}_{-0.02}$	$0.17^{+0.03}_{-0.02}$	$0.23^{+0.03}_{-0.03}$	$0.37^{+0.05}_{-0.04}$	$0.64^{+0.06}_{-0.06}$

interstellar radiation field (ISRF) is 6490 CU. Because the vantage point of G251.2+73.3 at $z = 120$ pc is above a large fraction of the Galactic dust layer, the lines of sight roughly parallel to the Galactic plane will have less extinction than for an observer located in the plane (Mattila 1980). Since the increase of the average ISRF intensity is expected to be small ($\lesssim 20\%$), we have decided, in view of the other uncertainties involved in estimating the ISRF, to adopt the values at the Sun's position.

4. DISCUSSION AND CONCLUSIONS

Comparison of the observed (H_2 fluorescence-subtracted) surface brightness excess $\Delta I = 335 \pm 75$ CU of G251.2+73.3 with the calculated values of Table 1 results in the best-fit albedo values for each assumed g-value as given in Table 2. Our results are seen to restrict the "allowed" domain of the scattering parameters into a narrow ridge in the (a, g)-plane, extending from $a = 0.13^{+0.04}_{-0.07}$ at $g = 0$ (isotropic scattering) to $a = 0.60^{+0.10}_{-0.14}$ at $g = 0.9$ (strong forward scattering). However, the nature of our data is such that it does not allow us to determine both a and g simultaneously. If we assume, following Hurwitz et al. (1991), that the grains scatter isotropically, then our albedo value is in good agreement with their result, $0.13 < a < 0.24$. On the other hand, if we assume that the grains have a strongly forward-scattering phase function, $g = 0.90$, as advocated recently, e.g., by Witt, et al. (1992) and Witt & Petersohn (1994), then our albedo value is in good agreement with the recent result of Witt & Petersohn (1994), $a = 0.5$, obtained from a reanalysis of the Fix, Craven, & Frank (1989) *Dynamics Explorer 1* data. Recently Henry & Murthy (1993) in a reanalysis of a part of the Berkeley and Johns Hopkins Ultraviolet Experiment (UVX) measurements, suggest boundaries to the range of allowed a- and g-values similar to those presented in Table 2.

In conclusion, our discovery and imaging of a Galactic cirrus cloud demonstrate that the radiation scattered by interstellar dust is an important constituent of the diffuse FUV background. The FUV intensity in the cloud is well correlated with two other dust column tracers: the far-IR intensity and the optical reddening. A Monte Carlo model for multiple scattering has been applied to our observational results to restrict the FUV scattering parameters of interstellar dust in the albedo–asymmetry parameter plane.

This research is supported in part by NASA contract NAS 8-32577 and the CNES Science Program. S. B. acknowledges support from the John Simon Guggenheim Memorial Foundation. IPAC provided us with the *IRAS* data. IPAC is funded by NASA as part of the *IRAS* extended mission program under contract to JPL.

REFERENCES

Bowyer, S. A. 1991, ARA&A, 29, 59
Bowyer, S., Sasseen, T. P., Lampton, M., & Wu, X. 1993, ApJ, 415, 875
Deul, E. R., & Burton, W. B. 1990, A&A, 230, 153
Fix, J. D., Craven, J. D., & Frank, L. A. 1989, ApJ, 345, 203
Gondhalekar, P. M. 1990, in IAU Symp. 139, The Galactic and Extragalactic Background Radiation, ed. S. Bowyer & Ch. Leinert (Dordrecht: Kluwer), 49
Gondhalekar, P. M., Phillips, A. P., & Wilson, R. 1980, A&A, 85, 272
Henry, R. C., & Murthy, J. 1993, ApJ, 418, L17
Henyey, L. G., & Greenstein, J. L. 1941, ApJ, 93, 70
Hurwitz, M., Bowyer, S., & Martin, C. 1991, ApJ, 372, 167
Jakobsen, P., de Vries, J. S., & Paresce, F. 1987, A&A, 183, 335
Knude, J. 1985, in Mat.-fys. Medd. 41, Kon. Dan. Vid. Selskab, 71
Laureijs, R. J., Chlewicki, G., Clark, F. O., & Wesselius, P. R. 1989, A&A, 220, 226
Laureijs, R. J., Mattila, K., & Schnur, G. 1987, A&A, 184, 269
Martin, C., Hurwitz, M., & Bowyer, S. 1990, ApJ, 354, 220
Mattila, K. 1970, A&A, 9, 53
———. 1976, A&A, 47, 77
———. 1980, A&A, 82, 373
Murthy, J., Henry, R. C., Feldman, P. D., & Tennyson, P. D. 1990, A&A, 231, 187
Palous, J., & Hauck, B. 1986, A&A, 162, 54
Pérault, M., Lequeux, J., Hanus, M., & Joubert, M. 1991, A&A, 246, 243
Sasseen, T. P., et al. 1994, ApJ, submitted
Seaton, M. J. 1979, MNRAS, 187, 73P
Witt, A. N., & Petersohn, J. K. 1994, in ASP Conf. Ser. 58, First Symposium on the Infrared Cirrus and Diffuse Interstellar Clouds, ed. R. Cutri & W. Latter (San Francisco: ASP), 91
Witt, A. N., Petersohn, J. K., Bohlin, R. C., O'Connell, R. W., Roberts, M. S., Smith, A. M., & Stecher, T. P. 1992, ApJ, 395, L5